NPRE 555
Computer Project 3

Roberto E. Fairhurst Agosta
ref3@illinois.edu

December 16, 2020

1 Introduction

For this project, I have implemented kernels in a MOOSE-based application to solve the SP3 transport method equations. This report presents the development of those kernels as well as results of one and two-dimensional models. Section 3.a displays the results of the one-dimensional model and compares them against the diffusion solver in Moltres [**?**]. Section 3.b presents the results of a two-dimensional model of the C5 MOX Benchmark [2].

2 Methodology

This section of the report introduces different software utilized in the development of this work.

2.a MOOSE

MOOSE [**?**] is a computational framework that supports engineering analysis applications. In a nuclear reactor, several partial differential equations describe the physical behavior. These equations are typically nonlinear, and they are often coupled to each other. Multi-physics Object-Oriented Simulation Environment (MOOSE) targets such systems and solves them in a fully coupled manner.

MOOSE is an open-source FEM framework. The framework itself relies on LibMesh [**?**] and PetSc [**?**] for solving nonlinear equations. MOOSE applications define weak forms of the governing equations and modularize the physics expressions into "kernels." Kernels are C++ classes containing methods for computing the residual and Jacobian contributions of individual pieces of the governing equations. MOOSE and LibMesh translate them into residual and Jacobian functions. These functions become inputs into PetSc solution routines.

All the software built on the MOOSE framework shares the same Application Programming Interface (API). The applications, by default, utilize implicit methods [**?**]. This feature facilitates relatively easy coupling between different phenomena [**?**]. Additionally, the framework and its applications use Message Passing Interface (MPI) for parallel communication and allow deployment on massively-parallel cluster-computing platforms.

2.b Simplified P_3

One dimensional P_3 equations [1]

$$\frac{d}{dx}\phi_{1,g} + \Sigma_{t,g}\phi_{0,g} = \sum_{g'=1}^{G} \Sigma_{s0,g'\to g}\phi_{0,g'} + \frac{\chi_g}{k_{eff}} \sum_{g'=1}^{G} \nu\Sigma_{f,g'}\phi_{0,g'} + Q_{0,g} \tag{1}$$

$$\frac{1}{3}\frac{d}{dx}\phi_{0,g} + \frac{2}{3}\frac{d}{dx}\phi_{2,g} + \Sigma_{t,g}\phi_{1,g} = \sum_{g'=1}^{G} \Sigma_{s1,g'\to g}\phi_{1,g'} + Q_{1,g} \tag{2}$$

$$\frac{2}{5}\frac{d}{dx}\phi_{1,g} + \frac{3}{5}\frac{d}{dx}\phi_{3,g} + \Sigma_{t,g}\phi_{2,g} = \sum_{g'=1}^{G} \Sigma_{s2,g'\to g}\phi_{2,g'} + Q_{2,g} \tag{3}$$

$$\frac{3}{7}\frac{d}{dx}\phi_{2,g} + \Sigma_{t,g}\phi_{3,g} = \sum_{g'=1}^{G} \Sigma_{s3,g'\to g}\phi_{3,g'} + Q_{3,g} \tag{4}$$

where

$\phi_{n,g} = n^{th}$ moment of the group g neutron flux $[n \cdot cm^{-2} \cdot s^{-1}]$
$\Sigma_{t,g}$ = group g macroscopic total cross-section $[cm^{-1}]$
$\Sigma_{sn,g' \to g} = n^{th}$ moment of the group g' to group g macroscopic scattering cross-section $[cm^{-1}]$
$\nu\Sigma_{f,g}$ = group g macroscopic production cross-section $[cm^{-1}]$
χ_g = group g fission spectrum $[cm^{-1}]$
k_{eff} = multiplication factor $[-]$
$Q_{n,g} = n^{th}$ group g external neutron source $[n \cdot cm^{-3} \cdot s^{-1}]$
G = number of energy groups $[-]$.

Defining the group g "removal" cross-section $\Sigma_{n,g}$, and assuming an isotropic external source and a negligible anisotropic group-to-group scattering [1]

$$\begin{aligned}
&\Sigma_{n,g} = \Sigma_{t,g} - \Sigma_{sn,g' \to g} \\
&Q_{n,g} = 0, \quad n > 0 \\
&\Sigma_{sn,g' \to g} = 0, \quad g' \neq g, \quad n > 0
\end{aligned}$$

the P_3 equations become

$$\frac{d}{dx}\phi_{1,g} + \Sigma_{0,g}\phi_{0,g} = \sum_{g' \neq g}^{G} \Sigma_{s0,g' \to g}\phi_{0,g'} + \frac{\chi_g}{k_{eff}} \sum_{g'=1}^{G} \nu\Sigma_{f,g'}\phi_{0,g'} + Q_{0,g} \tag{5}$$

$$\frac{1}{3}\frac{d}{dx}\phi_{0,g} + \frac{2}{3}\frac{d}{dx}\phi_{2,g} + \Sigma_{1,g}\phi_{1,g} = 0 \tag{6}$$

$$\frac{2}{5}\frac{d}{dx}\phi_{1,g} + \frac{3}{5}\frac{d}{dx}\phi_{3,g} + \Sigma_{2,g}\phi_{2,g} = 0 \tag{7}$$

$$\frac{3}{7}\frac{d}{dx}\phi_{2,g} + \Sigma_{3,g}\phi_{3,g} = 0. \tag{8}$$

Reorganizing equations 6 and 8 allows for obtaining a expression for odd moments of the flux $\phi_{1,g}$ and $\phi_{3,g}$

$$\phi_{1,g} = -\frac{1}{3\Sigma_{1,g}}\frac{d}{dx}\left[\phi_{0,g} + 2\phi_{2,g}\right] \tag{9}$$

$$\phi_{3,g} = -\frac{3}{7\Sigma_{3,g}}\frac{d}{dx}\phi_{2,g}. \tag{10}$$

With equations 9 and 10, equations 5 and 7 become

$$-D_{0,g}\frac{d^2}{dx^2}\left(\phi_{0,g} + 2\phi_{2,g}\right) + \Sigma_{0,g}\phi_{0,g} = \sum_{g' \neq g}^{G} \Sigma_{s0,g' \to g}\phi_{0,g'} + \frac{\chi_g}{k_{eff}} \sum_{g'=1}^{G} \nu\Sigma_{f,g'}\phi_{0,g'} + Q_{0,g} \tag{11}$$

$$-\frac{2}{5}D_{0,g}\frac{d^2}{dx^2}\left(\phi_{0,g} + 2\phi_{2,g}\right) - D_{2,g}\frac{d^2}{dx^2}\phi_{2,g} + \Sigma_{2,g}\phi_{2,g} = 0 \tag{12}$$

where

$$\begin{aligned}
D_{0,g} &= \frac{1}{3\Sigma_{1,g}} \\
D_{2,g} &= \frac{9}{35\Sigma_{3,g}}
\end{aligned}$$

Introducing the variables $\Phi_{0,g}$ and $\Phi_{2,g}$ and reorganizing equations 11 and 12 yields

$$-D_{0,g}\frac{d^2}{dx^2}\Phi_{0,g}+\Sigma_{0,g}\Phi_{0,g}-2\Sigma_{0,g}\Phi_{2,g}=S_{0,g} \tag{13}$$

$$-D_{2,g}\frac{d^2}{dx^2}\Phi_{2,g}+\left(\Sigma_{2,g}+\frac{4}{5}\Sigma_{0,g}\right)\Phi_{2,g}-\frac{2}{5}\Sigma_{0,g}\Phi_{0,g}=-\frac{2}{5}S_{0,g} \tag{14}$$

where

$$\Phi_{0,g}=\phi_{0,g}+2\phi_{2,g}$$
$$\Phi_{2,g}=\phi_{2,g}$$
$$S_{0,g}=\sum_{g'\neq g}^{G}\Sigma_{s0,g'\to g}\left(\Phi_{0,g'}-2\Phi_{2,g'}\right)+\frac{\chi_g}{k_{eff}}\sum_{g'=1}^{G}\nu\Sigma_{f,g'}\left(\Phi_{0,g'}-2\Phi_{2,g'}\right)+Q_{0,g}.$$

The three-dimensional SP3 equations [3] replace the second-derivatives in equations 13 and 14 by the Laplace operator Δ (See PARCS manual)

$$-D_{0,g}\Delta\Phi_{0,g}+\Sigma_{0,g}\Phi_{0,g}-2\Sigma_{0,g}\Phi_{2,g}=S_{0,g} \tag{15}$$

$$-D_{2,g}\Delta\Phi_{2,g}+\left(\Sigma_{2,g}+\frac{4}{5}\Sigma_{0,g}\right)\Phi_{2,g}-\frac{2}{5}\Sigma_{0,g}\Phi_{0,g}=-\frac{2}{5}S_{0,g}. \tag{16}$$

The Marshak vacuum boundary conditions complete the system of equations

$$\frac{1}{4}\Phi_{0,g}\pm\frac{1}{2}\hat{n}\cdot J_{0,g}-\frac{3}{16}\Phi_{2,g}=0 \tag{17}$$

$$-\frac{3}{80}\Phi_{0,g}\pm\frac{1}{2}\hat{n}\cdot J_{2,g}+\frac{21}{80}\Phi_{2,g}=0 \tag{18}$$

where

$$J_{n,g}=-D_{n,g}\nabla\Phi_{n,g}.$$

Variational formulation

$$\langle\Phi,\Psi\rangle=\int_V\Phi\Psi dV \tag{19}$$

$$\langle\Phi,\Psi\rangle_{BC}=\int_S\Phi\Psi dS \tag{20}$$

where

$\Psi=$ test function
$S=$ boundary surface.

$$\langle-D_{0,g}\Delta\Phi_{0,g},\Psi\rangle+\langle\Sigma_{0,g}\Phi_{0,g},\Psi\rangle+\langle-2\Sigma_{0,g}\Phi_{2,g},\Psi\rangle+\langle-S_{0,g},\Psi\rangle=0 \tag{21}$$

$$\langle-D_{2,g}\Delta\Phi_{2,g},\Psi\rangle+\left\langle\left(\Sigma_{2,g}+\frac{4}{5}\Sigma_{0,g}\right)\Phi_{2,g},\Psi\right\rangle+\left\langle-\frac{2}{5}\Sigma_{0,g}\Phi_{0,g}D_{2,g},\Psi\right\rangle+\left\langle\frac{2}{5}S_{0,g},\Psi\right\rangle=0. \tag{22}$$

By means of the Gauss theorem (?), equations 24 and 26 become

$$\langle D_{0,g}\nabla\Phi_{0,g},\nabla\Psi\rangle+\langle -D_{0,g}\nabla\Phi_{0,g},\Psi\rangle_{BC}+\langle\Sigma_{0,g}\Phi_{0,g},\Psi\rangle+\langle -2\Sigma_{0,g}\Phi_{2,g},\Psi\rangle \tag{23}$$

$$+\left\langle -\sum_{g'\neq g}^{G}\Sigma_{s0,g'\to g}\left(\Phi_{0,g'}-2\Phi_{2,g'}\right),\Psi\right\rangle+\left\langle -\frac{\chi_g}{k_{eff}}\sum_{g'=1}^{G}\nu\Sigma_{f,g'}\left(\Phi_{0,g'}-2\Phi_{2,g'}\right),\Psi\right\rangle+\langle -Q_{0,g},\Psi\rangle=0 \tag{24}$$

$$\langle D_{2,g}\nabla\Phi_{2,g},\nabla\Psi\rangle+\langle -D_{2,g}\nabla\Phi_{2,g},\Psi\rangle_{BC}+\left\langle\left(\Sigma_{2,g}+\frac{4}{5}\Sigma_{0,g}\right)\Phi_{2,g},\Psi\right\rangle+\left\langle -\frac{2}{5}\Sigma_{0,g}\Phi_{0,g},\Psi\right\rangle \tag{25}$$

$$+\left\langle\frac{2}{5}\sum_{g'\neq g}^{G}\Sigma_{s0,g'\to g}\left(\Phi_{0,g'}-2\Phi_{2,g'}\right),\Psi\right\rangle+\left\langle\frac{2}{5}\frac{\chi_g}{k_{eff}}\sum_{g'=1}^{G}\nu\Sigma_{f,g'}\left(\Phi_{0,g'}-2\Phi_{2,g'}\right),\Psi\right\rangle+\left\langle\frac{2}{5}Q_{0,g},\Psi\right\rangle=0. \tag{26}$$

Vacuum BCs kernels?

$$\langle -D_{0,g}\nabla\Phi_{0,g},\Psi\rangle_{BC}=\left\langle -\frac{1}{2}\Phi_{0,g}+\frac{3}{4}\Phi_{2,g},\Psi\right\rangle_{BC} \tag{27}$$

$$\langle -D_{2,g}\nabla\Phi_{2,g},\Psi\rangle_{BC}=\left\langle\frac{3}{40}\Phi_{0,g}-\frac{21}{40}\Phi_{2,g},\Psi\right\rangle_{BC} \tag{28}$$

$$\tag{29}$$

Table 1: .

Kernel	Equation A	Equation B
P3Diffusion	$\langle D_{0,g}\nabla\Phi_{0,g},\nabla\Psi\rangle$	$\langle D_{2,g}\nabla\Phi_{2,g},\nabla\Psi\rangle$
P3SigmaR	$\langle\Sigma_{0,g}\Phi_{0,g},\Psi\rangle$	$\left\langle\left(\Sigma_{2,g}+\frac{4}{5}\Sigma_{0,g}\right)\Phi_{2,g},\Psi\right\rangle$
P3SigmaCoupled	$\langle -2\Sigma_{0,g}\Phi_{2,g},\Psi\rangle$	$\left\langle -\frac{2}{5}\Sigma_{0,g}\Phi_{0,g},\Psi\right\rangle$
P3InScatter	$\left\langle -\sum_{g'\neq g}^{G}\Sigma_{s0,g'\to g}\left(\Phi_{0,g'}-2\Phi_{2,g'}\right),\Psi\right\rangle$	$\left\langle\frac{2}{5}\sum_{g'\neq g}^{G}\Sigma_{s0,g'\to g}\left(\Phi_{0,g'}-2\Phi_{2,g'}\right),\Psi\right\rangle$
P3FissionEigenKernel	$\left\langle -\frac{\chi_g}{k_{eff}}\sum_{g'=1}^{G}\nu\Sigma_{f,g'}\left(\Phi_{0,g'}-2\Phi_{2,g'}\right),\Psi\right\rangle$	$\left\langle\frac{2}{5}\frac{\chi_g}{k_{eff}}\sum_{g'=1}^{G}\nu\Sigma_{f,g'}\left(\Phi_{0,g'}-2\Phi_{2,g'}\right),\Psi\right\rangle$
Boundary Condition Kernel	**Equation A**	**Equation B**
Vacuum	$\left\langle -\frac{1}{2}\Phi_{0,g}+\frac{3}{4}\Phi_{2,g},\Psi\right\rangle_{BC}$	$\left\langle\frac{3}{40}\Phi_{0,g}-\frac{21}{40}\Phi_{2,g},\Psi\right\rangle_{BC}$

2.c Moltres

Moltres is a MOOSE-based application initially designed for modeling fluid-fuelled Molten Salt Reactors (MSRs). Moltres inherits all the attributes from MOOSE as its application. Moltres solves arbitrary-group neutron diffusion, delayed neutron precursor concentration, and temperature governing equations. It can solve the equations in a fully-coupled way or solve each system independently, allowing for great flexibility and making it applicable to a wide range of nuclear engineering problems. The development of this work utilized Moltres as a stand-alone neutronics solver, which calculates the scalar flux and the multiplication factor with the following equation

$$\nabla\cdot D_g\nabla\phi_g-\Sigma_g^r\phi_g+\sum_{g'\neq g}^{G}\Sigma_{g'\to g}^{s}\phi_{g'}+\chi_g^t\sum_{g'=1}^{G}\frac{1}{k_{eff}}\nu\Sigma_{g'}^{f}\phi_{g'}+Q_g=0 \tag{30}$$

where

D_g = group g diffusion coefficient $[cm]$
ϕ_g = group g neutron flux $[n \cdot cm^{-2} \cdot s^{-1}]$
Σ_g^r = group g macroscopic removal cross-section $[cm^{-1}]$
$\Sigma_{g' \to g}^s$ = group g' to group g macroscopic scattering cross-section $[cm^{-1}]$
χ_t^p = group g total fission spectrum $[-]$
G = number of discrete energy groups $[-]$
k_{eff} = multiplication factor $[-]$
ν = number of neutrons produced per fission $[-]$
Σ_g^f = group g macroscopic fission cross-section $[cm^{-1}]$. Q_g = group g external neutron

2.d C5 MOX Benchmark

The Organisation for Economic Co-operation and Development (OECD)/Nuclear Energy Agency (NEA) developed this benchmark to carry out validation of methods and identify their strengths, limitations, and accuracy, and to suggest needs for method development. The definition of the original benchmark can be found in [4]. Capilla et al [2] developed a simplified version of the benchmark using a two-energy group structure.

Figures 1 and 2 display the configuration of the benchmark exercise. Tables 2 and 3 present the group constants necessary to carry out the exercise.

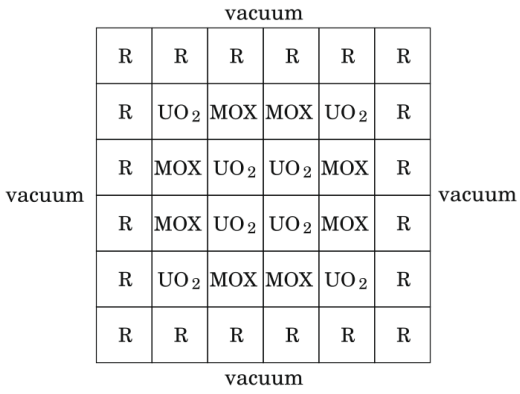

Figure 1: 2-D C5 MOX benchmark configuration. Image reproduced from [2].

3 Results

3.a 1-D test case

Figure 3 displays the neutron flux for one and three energy groups for a fixed source case. Figure 4 shows the neutron flux for one and three energy groups for an eigenvalue problem. Table 4 compares the eigenvalue obtained with the SP3 and the diffusion solvers by calculating their difference with the formula

$$\Delta_\rho = |\rho_{P_3} - \rho_{Ref}| = \left| \frac{k_{P_3} - 1}{k_{P_3}} - \frac{k_{Ref} - 1}{k_{Ref}} \right| = \left| \frac{k_{P_3} - k_{Ref}}{k_{P_3} k_{Ref}} \right| \tag{31}$$

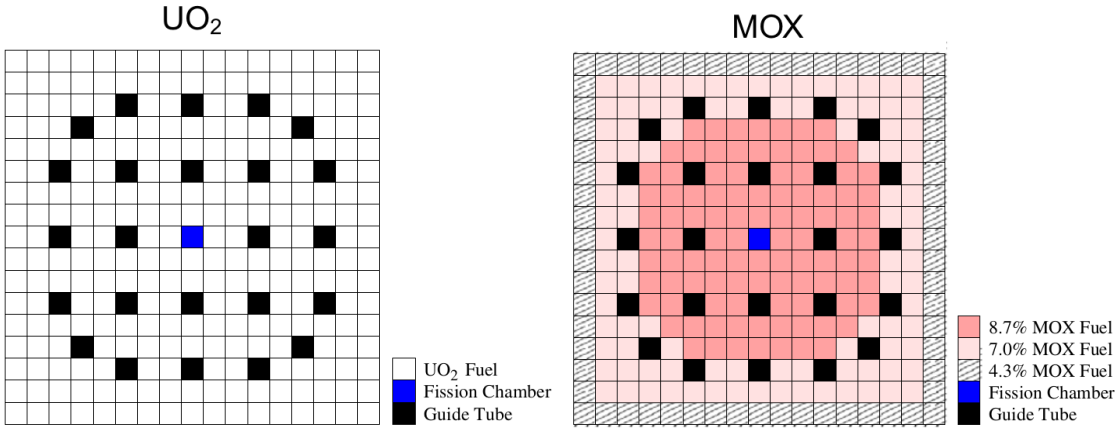

(a) UO_2 assembly.

(b) MOX assembly.

Figure 2: Structure of the UO_2 and MOX assemblies. Images reproduced from [2].

Table 2: Two-group cross-sections $[cm^{-1}]$ for the heterogeneous problem.

Pin cell type	Group	Σ_t	$\nu\Sigma_f$	$\Sigma_{s0,1\to g}$	$\Sigma_{s0,2\to g}$
4.3% MOX	1	0.550	0.0075	0.520	0.000
	2	1.100	0.3000	0.015	0.900
7.0% MOX	1	0.550	0.0075	0.520	0.000
	2	1.010	0.3750	0.015	0.760
8.7% MOX	1	0.550	0.0075	0.520	0.000
	2	1.060	0.4500	0.015	0.760
UO_2	1	0.570	0.0050	0.540	0.000
	2	1.100	0.1250	0.020	1.000
Guide tube	1	0.586	0.0000	0.560	0.000
	2	1.220	0.0000	0.025	1.200
Reflector	1	0.611	0.0000	0.560	0.000
	2	2.340	0.0000	0.050	2.300
Fission chamber	1	0.586	10^{-7}	0.560	0.000
	2	1.220	3×10^{-6}	0.025	1.200

Table 3: Two-group cross-sections $[cm^{-1}]$ for the heterogeneous problem.

Pin cell type	Group	Σ_t	$\nu\Sigma_f$	$\Sigma_{s0,1\to g}$	$\Sigma_{s0,2\to g}$
MOX	1	0.553087	0.006857	0.523430	0.000000
	2	1.068911	0.340391	0.016089	0.839806
UO_2	1	0.571360	0.004575	0.541700	0.000000
	2	1.111391	0.113135	0.020475	1.018984

where

$$k_{P_3} = \text{eigenvalue obtained with SP3 solver}[-]$$
$$k_{Ref} = \text{eigenvalue obtained with diffusion solver}[-].$$

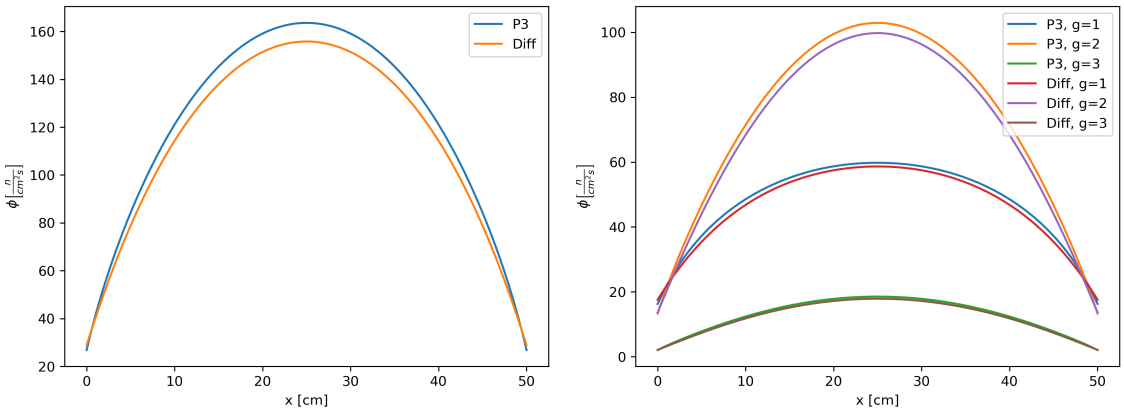

(a) 1 group. (b) 3 groups.

Figure 3: Comparison of the scalar flux obtained with the SP3 and diffusion solvers for the fixed source case.

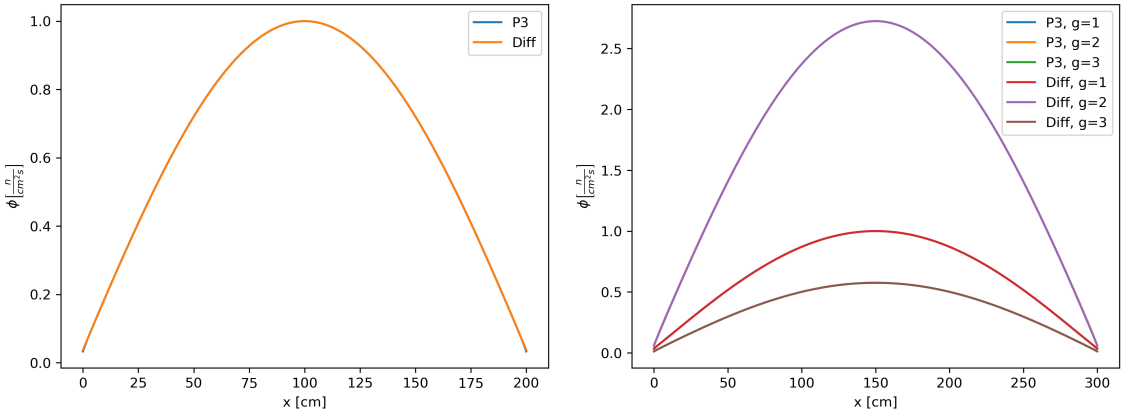

(a) 1 group. (b) 3 groups.

Figure 4: Comparison of the scalar flux obtained with the SP3 and diffusion solvers for the eigenvalues problem.

Table 4: Comparison between the eigenvalue obtained with the SP3 and diffusion solvers.

	Moltres	P3	
	k_{eff}	k_{eff}	Δ_ρ [pcm]
1	1.05278	1.06004	650
3	1.02878	1.03005	21

3.b 2-D test case

Figure 5 displays the scalar flux of the C5G2 MOX Benchmark. Table 5 compares the eigenvalue obtained with the SP3 solver (k_{P_3}) and the results in [2] (k_{Ref}) by using equation 31.

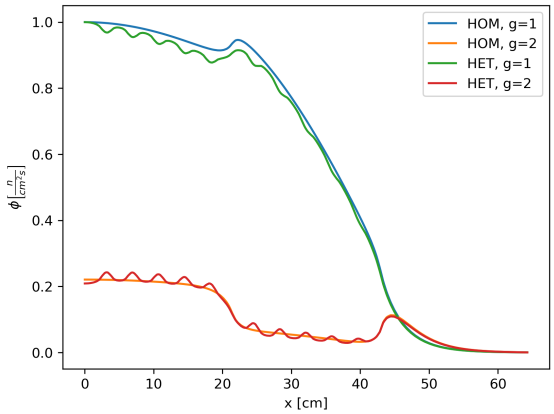

Figure 5: Scalar flux on line between points (0, 10.71) and (64.26, 10.71). HOM: homogeneous case, HET: heterogeneous case.

Table 5: Comparison between the eigenvalue obtained with the SP3 solver and the results in [2].

	C5G2 Benchmark	P3	
	k_{Ref}	k_{eff}	Δ_ρ [pcm]
Heterogeneous	0.96969	0.97106	145
Homogeneous	0.96983	0.97761	821

4 Conclusions

References

[1] P.S. Brantley and E.W. Larsen. The Simplified P3 Approximation. *Nuclear Science and Engineering*, 2000.

[2] M. Capilla, D. Ginestar, and G. Verdú. Applications of the multidimensional equations to complex fuel assembly problems. *Annals of Nuclear Energy*, 36(10):1624–1634, October 2009.

[3] E.M. Gelbard. Application of spherical harmonics methods to reactor problems. Technical Report WAPD-BT-20, Bettis Atomic Power Laboratory, 1960.

[4] OECD/NEA. Benchmark on Deterministic Transport Calculations Without Spatial Homogenisation: A 2-D/3-D MOX Fuel Assembly Benchmark. Technical Report NEA/NSC/DOC(2003)16, OECD, 2003.